Improving total column ozone retrievals by using cloud pressures derived from Raman scattering in the UV

Alexander P. Vasilkov,[1] Joanna Joiner,[2] Kai Yang,[1] and Pawan K. Bhartia[2]

Received 25 May 2004; revised 9 August 2004; accepted 29 September 2004; published 27 October 2004.

[1] The higher spectral resolution, coverage, and sampling of the Aura satellite ozone monitoring instrument (OMI), as compared with the total ozone mapping spectrometer (TOMS) should allow for improved ozone retrievals. By default, the TOMS-like OMI total column ozone algorithm uses climatological cloud-top pressures based on infrared (IR) measurements to estimate the column ozone below the clouds. Alternatively, cloud pressure can be retrieved using atmospheric rotational Raman scattering. The retrieved cloud pressures should be more consistent with assumptions made in the total ozone algorithm. Here, we use data from the global ozone monitoring experiment (GOME) to estimate total ozone using both the IR-climatological and retrieved cloud pressures. The resulting ozone differences can be significant but do not exceed ~15 DU. Use of the cloud pressure retrievals leads to a smoother distribution of ozone along a satellite track by reducing small spatial irregularities presumably caused by the difference between the retrieved and climatological cloud pressures. *INDEX TERMS:* 0320 Atmospheric Composition and Structure: Cloud physics and chemistry; 0360 Atmospheric Composition and Structure: Transmission and scattering of radiation; 3360 Meteorology and Atmospheric Dynamics: Remote sensing. **Citation:** Vasilkov, A. P., J. Joiner, K. Yang, and P. K. Bhartia (2004), Improving total column ozone retrievals by using cloud pressures derived from Raman scattering in the UV, *Geophys. Res. Lett.*, *31*, L20109, doi:10.1029/2004GL020603.

1. Introduction

[2] Cloud pressure estimates are needed for the retrieval of ozone and other trace gases using satellite-borne backscatter UV instruments in cloudy conditions. Errors in the assumed cloud pressure can produce non-negligible errors in retrieved total column ozone [*Koelemeijer and Stammes*, 1999]. The TOMS retrieval algorithm uses a cloud pressure climatology from the international satellite cloud climatology project (ISCCP) [*Rossow and Schiffer*, 1991] that is based on thermal IR satellite data.

[3] Advanced spectrometers such as the GOME, flying on ESA's environmental research satellite 2 (ERS-2) satellite, the scanning imaging absorption spectrometer for atmospheric chartography (SCIAMACHY), flying on the ESA Envisat satellite, and the OMI, flying on NASA's Earth Observing System Aura satellite, have better spectral coverage that enables the retrieval of cloud pressure using approaches based on gaseous absorption in narrow bands and rotational Raman scattering (RRS). These techniques are based on the fact that clouds screen the atmosphere below from satellite observations. Therefore, clouds reduce the amount of RRS and absorption seen by satellite-borne instruments. Examples of these methods include cloud pressures retrievals based on RRS [*Joiner and Bhartia*, 1995], absorption in the O_2 A band at 762 nm [*Koelemeijer et al.*, 2001], and in the O_2-O_2 band near 477 nm [*Acarreta et al.*, 2004]. GOME contains spectral bands applicable to all three of these methods, while OMI's more limited spectral range does not include O_2 A band wavelengths.

[4] An effective cloud pressure can be defined using the concept of a Lambert-equivalent reflectivity (LER) surface. The LER concept is also used in many trace gas retrieval algorithms including the TOMS total ozone algorithm. It has been shown that using IR-derived cloud-top pressures produces errors in retrieved total column ozone if clouds are treated as Lambertian. This is due to unaccounted for ozone absorption within clouds [*Newchurch et al.*, 2001].

[5] Cloud pressures are also needed to study long-term and seasonal variations in tropical tropospheric ozone derived from cloud slicing techniques [e.g., *Ziemke et al.*, 2001] and the convective-cloud differential method [*Ziemke et al.*, 1998]. These methods have been implemented using IR cloud-top pressures or other assumptions about clouds. The use of retrieved LER cloud pressures may significantly improve the tropospheric ozone estimated by these methods and extend their range to higher latitudes.

[6] In this paper, we analyze total column ozone differences that result from replacing the IR-based climatological cloud-top pressures with those retrieved by the RRS method based on *Joiner et al.* [2004].

2. GOMI Data

[7] We use data from the available orbits of 24 March 1998. On this day, GOME was operated in the small pixel mode where the ground pixel size was 40 by 80 km^2. The GOME data has been modified to look like OMI data to facilitate the utilization of software developed for the OMI. The modified data will be referred to as GOMI data. These modifications include convolving the radiances with the OMI spectral response function and resampling to OMI wavelengths (P. Veefkind, personal communication, 2004). Due to potential problems with the GOMI off-nadir observations, we use only nadir observations. In this work, we use the OMI operational software developed for the retrieval of cloud pressure

[1]Science Systems and Applications, Inc., Lanham, Maryland, USA.
[2]NASA Goddard Space Flight Center, Greenbelt, Maryland, USA.

0094-8276/04/2004GL020603$05.00

based on RRS and for total ozone based on the TOMS Version 8 (V8) algorithm.

3. The OMI UV Cloud Pressure Algorithm

[8] The details of the RRS cloud pressure algorithm are described in *Joiner et al.* [2004]. Briefly, cloud pressure is retrieved using an iterative minimum-variance approach with wavelengths between 355 and 365 nm. The cloud pressure is determined only from the high-frequency component of observed reflectance that is due to filling-in of Fraunhofer lines by atmospheric RRS. Calculations of RRS filling-in are based on *Joiner et al.* [1995]. In this study, we do not account for ocean Raman scattering [*Vasilkov et al.*, 2002], because we use only scenes that are likely to be significantly cloud covered.

[9] The UV OMI cloud pressure algorithm makes use of a mixed LER approach: The LER assumption is combined with the independent pixel approximation given by

$$I_m = (1-f)I_{\mathrm{Clr}} + fI_{\mathrm{Cld}}, \quad (1)$$

where I_m is the measured radiance, f is the cloud fraction, I_{Clr} and I_{Cld} are the clear-scene and cloudy-scene radiances respectively. Those radiances are estimated using assumed values of clear (ground) and cloudy reflectivities, R_{Clr} and R_{Cld}. Then the cloud fraction is calculated from equation (1). To be consistent with the OMI total ozone algorithm, which also uses the mixed LER approach, we assume R_{Clr} = 15% and R_{Cld} = 80%. The value of R_{Clr} was selected to account for the effects of aerosol [*Bhartia and Wellemeyer*, 2002].

4. The TOMS Version 8 Total Ozone Algorithm

[10] The TOMS V8 algorithm [*Bhartia and Wellemeyer*, 2002] is used to retrieve the total column ozone amount in a three-step process. First, a guess value of total ozone is derived using radiances at a pair of wavelengths (318 and 331 nm). The radiances are calculated using standard ozone and temperature profiles for the measurement geometries and surface conditions specified by cloud and terrain pressures, and surface type. Second, climatological ozone and temperature profiles are used to improve the radiance calculations by accounting for the seasonal and latitudinal variations. Finally the retrieved ozone is modified to correct for various effects including "hidden" ozone beneath clouds, tropospheric aerosol, sun glint, and errors in the upper level profile shape. The correction for "hidden" ozone is applied using an assumed tropospheric ozone profile and an estimated cloud top pressure. By default, the total ozone algorithm uses the ISCCP cloud-top pressure climatology (p_{clim}). As a second option, we use cloud pressures from the OMI UV algorithm (p_{ret}). For snow/ice pixels, the total ozone algorithm assumes cloud-free conditions. Therefore, we exclude these pixels from our analysis.

[11] *Newchurch et al.* [2001] identified three types of errors associated with cloud-top height: 1) radiance interpolation error, 2) ozone retrieval error above cloud, and 3) ozone retrieval error below cloud. The first error was eliminated in the V8 total ozone algorithm by using four pressure levels for computations of radiances instead of the two in V7. The second error can be reduced when retrieved cloud pressures replace climatological cloud pressures. The third error can also be reduced by using retrieved cloud pressures. However, errors may still occur if the assumed tropospheric ozone mixing ratios are incorrect. Errors due to treating the clouds as opaque Lambertian surfaces and using the independent pixel approximation remain.

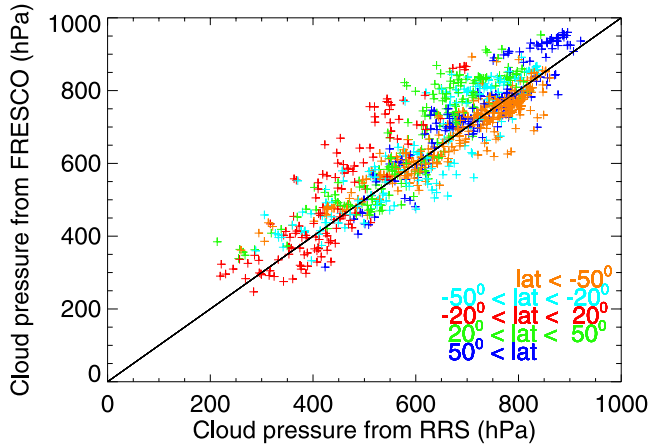

Figure 1. Cloud pressures from the FRESCO versus p_{ret} along with the 1:1 line for all orbits of 24 March 1998 for $R > 40\%$.

5. Results With GOMI Data

[12] *Joiner et al.* [2004] compared p_{ret} from GOME data with cloud-top pressures derived from thermal IR observations from the along track scanning radiometer – 2 (ATSR-2) that also flies on board ERS-2 also for 24 March 1998. This comparison showed that p_{ret} was consistently higher than the estimated cloud top from ATSR-2. The bias was ~200 hPa and the correlation coefficient was 0.8. Here, we compare rotational-Raman (RR) pressures, p_{ret}, (from GOMI data) with cloud pressures derived by the fast retrieval scheme for clouds from the oxygen A-band (FRESCO) algorithm [*Koelemeijer et al.*, 2001] using GOME data in Figure 1. We focus exclusively on scenes with Lambert-equivalent reflectivity, $R > 40\%$, where a pixel is likely to be significantly cloud covered. The agreement between two algorithms is good, although there are some geographical dependencies. There is less of a bias with respect to FRESCO than with the thermal ATSR-2 cloud-tops and the correlation is higher. This may be due to the fact that absorption and RRS retrievals both have their basis in cloud screening effects, which is fundamentally different than thermal emission.

[13] Table 1 gives statistics for the comparison for two cases: $R > 40\%$ and $R > 60\%$. The latter case assures the scenes are more cloud covered thus avoiding a potential problem due to different retrieved cloud fractions. This problem may result from different assumptions about R_{Clr} and its actual characteristics. Table 1 contains a bias defined as a difference between mean values, the root mean squared (RMS) difference, the correlation coefficient, and the slope of linear regression of FRESCO/Climatology pressures versus RR pressures. As expected, the correlation coeffi-

Table 1. Statistics for the Rotational-Raman and FRESCO/Climatology Pressure Comparison[a]

	FRESCO		Climatology	
	$R > 40\%$	$R > 60\%$	$R > 40\%$	$R > 60\%$
No. pixels	974	433	974	433
Bias (hPa)	−26.5	8.5	73.2	85.4
RMS (hPa)	66.7	51.3	121.0	103.2
Correlation	0.905	0.950	0.604	0.739
Slope	0.935	1.014	0.434	0.532

[a]See text.

cient is significantly higher for the FRESCO pressures than for the climatological pressures. It is also higher for scenes with $R > 60\%$ than for scenes with $R > 40\%$. The slope of linear regression of the FRESCO pressures versus RR pressures is almost equal to 1.0 and the bias is negligible for scenes with $R > 60\%$ thus proving a very good agreement between two algorithms when cloud fraction differences are minimized.

[14] Figure 2 shows a similar comparison of p_{ret} with p_{clim}. In the thermal IR, most clouds are optically thick and act as black-bodies. Therefore, the IR satellite measurements are primarily sensitive to the physical cloud-top. UV and visible satellite measurements derive an effective cloud pressure that is more indicative of the middle of the cloud [e.g., *Joiner et al.*, 2004; *Acarreta et al.*, 2004]. This is because the solar light penetration depth is comparable with the cloud physical thickness. Therefore, we may expect p_{ret} to be higher on average than p_{clim} as is shown in Figure 2. As may also be expected, the correlation between p_{ret} and p_{clim} is poor in all latitudinal bins as actual clouds are much more variable than a climatological average.

[15] Figure 3 shows the difference in total ozone retrievals, $\Delta\Omega = \Omega(p_{ret}) - \Omega(p_{clim})$, caused by replacing p_{clim} with p_{ret} versus the cloud pressure difference, $\Delta p = p_{ret} - p_{clim}$. $\Delta\Omega$ can be significant but does not exceed ~15 DU. It is interesting to note that the slope of $\Delta\Omega$ versus Δp varies with geographic area due to differences in the ozone profile as well as the cloud pressures. As expected, Δp is mostly positive resulting in negative $\Delta\Omega$ because lower clouds produce less "hidden" ozone.

[16] Our goal is to show that the use of p_{ret} improves the estimate of ozone above the clouds. One way to demonstrate this improvement is to examine the local homogeneity of $\Omega(p_{ret})$, which also includes hidden ozone added below the clouds. Our basic assumption is that the horizontal distribution of ozone above the clouds is homogeneous on small spatial scales. Then, when the hidden ozone is added below the cloud (using standard profiles), total ozone should be more spatially smooth when accurate cloud pressures are used. In other words, spatial irregularities of $\Omega(p_{clim})$ are presumably caused by errors in p_{clim}. Of course, spatial irregularities in total ozone can result from real small-scale geophysical events, e.g., by intrusion of stratospheric ozone into the troposphere. This should be seen in the tropics when there is significant observational sensitivity to tropospheric ozone, i.e., where there are no clouds, broken clouds, or clouds with lower to middle tropospheric pressures.

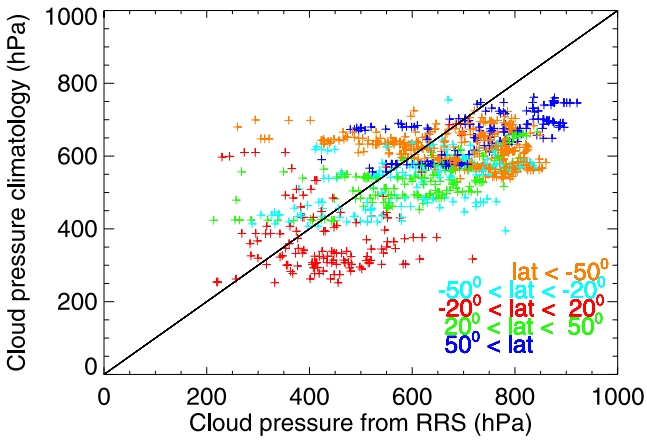

Figure 2. Similar to Figure 1 but showing scatter of p_{ret} vs. p_{clim}.

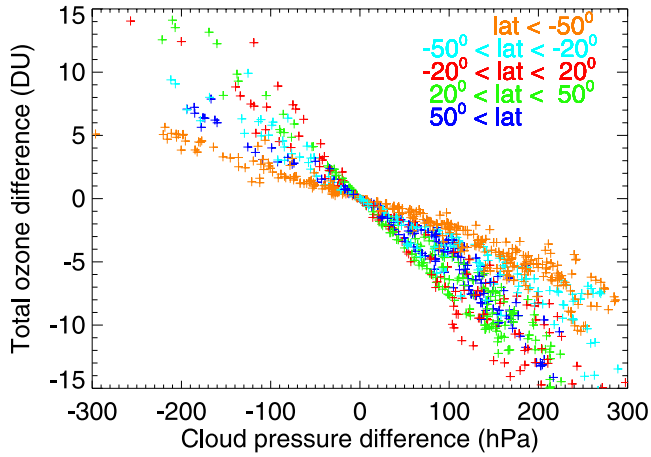

Figure 3. $\Delta\Omega$ versus Δp for all orbits and $R > 0.4$.

[17] First, we examine retrieved total ozone in the tropics where stratospheric variability is expected to be low. In the tropics highly reflective clouds tend to occur in convective regions and can extend to the tropopause. Therefore, the ozone above the clouds seen by the satellite in these pixels is primarily stratospheric.

[18] Figure 4 shows total ozone in the tropics as a function of reflectivity at 331 nm. The variance of $\Omega(p_{clim})$ does not

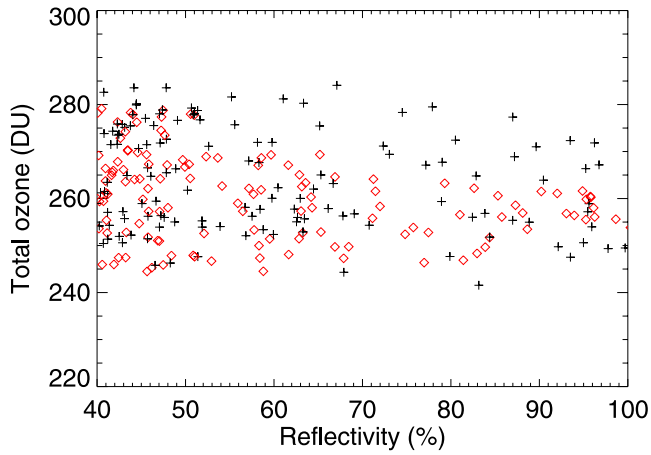

Figure 4. Diamonds: $\Omega(p_{ret})$ vs. R at 331 nm for latitudes between 20°S and 20°N. Plus signs: Similar but for $\Omega(p_{clim})$.

change noticeably with R. However, the variance of $\Omega(p_{ret})$ is significantly reduced as R increases. The lack of reduction in variance at lower reflectivities is attributed to the instrument sensing more ozone in the troposphere where small-scale variability has been observed [e.g., *Randriambelo et al.*, 2003]. At these lower reflectivities, it is likely that the clouds are occurring at lower altitudes and/or may be broken so that portions of the pixel are clear. The effect of reducing the ozone variability at the higher reflectivities is a strong indication that p_{ret} is more appropriate than p_{clim} for use in estimating ozone above clouds, and therefore for deriving tropospheric ozone by cloud slicing methods.

[19] Second, we examine the spatial distribution of total ozone at higher latitudes along a satellite track in Figures 5 and 6. When p_{ret} is used, the ozone distribution becomes smoother, i.e. bumps presumably caused by errors in p_{clim} disappear. If we assume a horizontally uniform distribution of tropospheric ozone, then a cloud pressure change will result in increased or reduced ozone depending on a sign of the difference. If the ozone mixing ratios above the clouds are relatively constant within the area of these bumps, then more accurate cloud pressures should have the effect of smoothing the total ozone distribution. Note that we do not claim $\Omega(p_{ret})$ is closer to real ozone because the hidden amount of ozone under the cloud may be in error.

6. Conclusions

[20] We have shown that replacing the default climatological cloud pressure derived from thermal IR measurements by the retrieved cloud pressure improves retrievals of ozone above clouds for scenes with reflectivity greater than 40%. Small-scale spatial irregularities presumably caused by differences between the retrieved and climatological cloud pressures are reduced. The smoothing effect is observed in the tropics over highly reflective clouds and at higher latitudes along satellite tracks in most GOME orbits. Future work will include deriving tropospheric ozone with retrieved cloud pressures from OMI. We also plan to produce a new cloud pressure climatology that will be more appropriate for applications that use the LER assumption such as trace gas retrievals from UV and visible instruments.

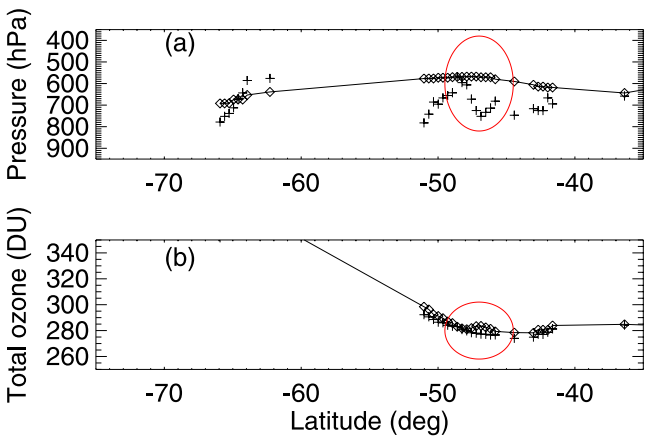

Figure 5. Smoothing of Ω along an orbital track around 47°S (circled) for GOME orbit 15288. Plus sign: p_{ret}, Diamond: p_{clim}.

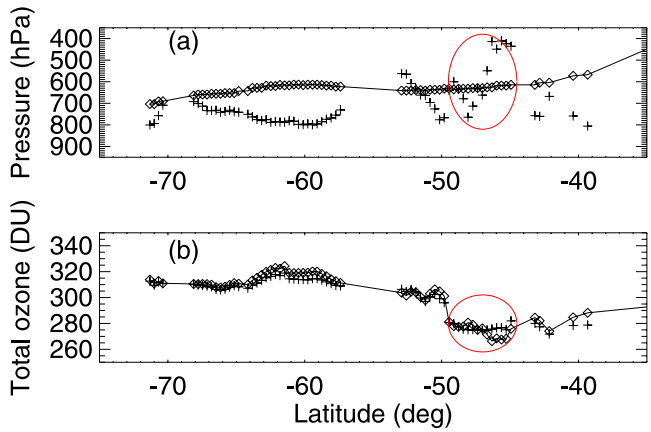

Figure 6. Similar to Figure 5 but for GOME orbit 15298.

This new climatology could be used in future reprocessing of the TOMS archived data.

[21] **Acknowledgments.** This work was performed under NASA contract NAS5-00220. We are grateful to Dr. J. de Haan who provided us with FRESCO data.

References

Acarreta, J. R., J. F. de Haan, and P. Stammes (2004), Cloud pressure retrieval using the O2-O2 absorption band at 477 nm, *J. Geophys. Res.*, *109*, D05204, doi:10.1029/2003JD003915.

Bhartia, P. K., and C. W. Wellemeyer (2002), TOMS-V8 Total O3 Algorithm, OMI Algorithm theoretical basis document, vol. 2, report, edited by P. K. Bhartia, NASA Goddard Space Flight Cent., Greenbelt, Md.

Joiner, J., and P. K. Bhartia (1995), The determination of cloud pressures from rotational-Raman scattering in satellite backscatter ultraviolet measurements, *J. Geophys. Res.*, *100*, 23,019–23,026.

Joiner, J., P. K. Bhartia, R. P. Cebula et al. (1995), Rotational-Raman scattering (Ring effect) in satellite backscatter ultraviolet measurements, *Appl. Opt.*, *34*, 4513–4525.

Joiner, J., A. P. Vasilkov, D. E. Flittner et al. (2004), Retrieval of cloud pressure and oceanic chlorophyll content using Raman scattering in GOME ultraviolet spectra, *J. Geophys. Res.*, *109*, D01109, doi:10.1029/2003JD003698.

Koelemeijer, R. B. A., and P. Stammes (1999), Effects of clouds on ozone column retrieval from GOME UV measurements, *J. Geophys. Res.*, *104*, 8281–8294.

Koelemeijer, R. B. A., P. Stammes, J. W. Hovenier, and J. F. de Haan (2001), A fast method for retrieval of cloud parameters using oxygen A band measurements from the GOME, *J. Geophys. Res.*, *106*, 3475–3490.

Newchurch, M. J., X. Liu, J. H. Kim, and P. K. Bhartia (2001), On the accuracy of Total Ozone Mapping Spectrometer retrievals over tropical cloudy regions, *J. Geophys. Res.*, *106*, 32,315–32,326.

Randriambelo, T., J. L. Baray, S. Baldy et al. (2003), Investigation of the short-time variability of tropical tropospheric ozone, *Ann. Geophys.*, *21*, 2095–2106.

Rossow, W. B., and R. A. Schiffer (1991), ISCCP cloud data products, *Bull. Am. Meteorol. Soc.*, *72*, 2–20.

Vasilkov, A. P., J. Joiner, J. Gleason, and P. K. Bhartia (2002), Ocean Raman scattering in satellite backscatter UV measurements, *Geophys. Res. Lett.*, *29*(17), 1837, doi:10.1029/2002GL014955.

Ziemke, J. R., S. Chandra, and P. K. Bhartia (1998), Two new methods for deriving tropospheric column ozone from TOMS measurements: Assimilated UARS MLS/HALOE and convective-cloud differential techniques, *J. Geophys. Res.*, *103*, 22,115–22,127.

Ziemke, J. R., S. Chandra, and P. K. Bhartia (2001), "Cloud slicing": A new technique to derive upper tropospheric ozone from satellite measurements, *J. Geophys. Res.*, *106*, 9853–9867.

P. K. Bhartia and J. Joiner, NASA Goddard Space Flight Center, Greenbelt, MD 20771, USA.

A. P. Vasilkov and K. Yang, Science Systems and Applications, Inc., 10210 Greenbelt Road, Suite 400, Lanham, MD 20706, USA. (alexander_vassilkov@ssaihq.com)